AD-A058 476 PENNSYLVANIA STATE UNIV UNIVERSITY PARK APPLIED RESE--ETC F/G 17/1
THE EFFECTS OF CLIPPING ON LINEAR BEAMFORMING WITH SINUSOIDAL I--ETC(U).
FEB 77 A E BREIHOLZ N00017-73-C-1418
UNCLASSIFIED ARL/PSU/TM-77-94 NL

1 OF 1
AD A058 476

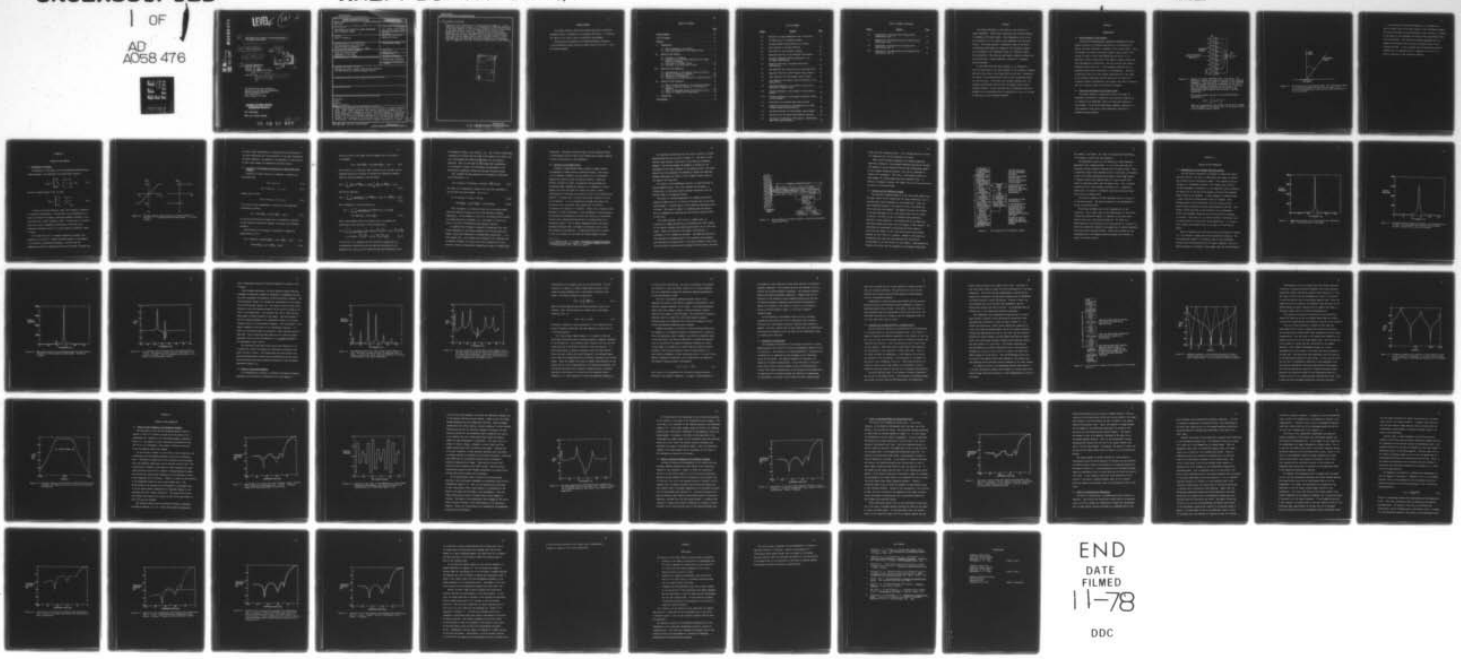

END
DATE FILMED
11-78
DDC

LEVEL II (12)

(6) THE EFFECTS OF CLIPPING ON LINEAR BEAMFORMING WITH SINUSOIDAL INPUTS.

(10) Arlen E. Breiholz

(13) 63p.

(11) 14 Feb 77

(9) Technical Memorandum
File No. TM 77-94
February 14, 1977
Contract No. N00017-73-C-1418

(15)

Copy No. 16

(14) ARL/PSU/TM-77-94

The Pennsylvania State University
Institute for Science and Engineering
APPLIED RESEARCH LABORATORY
Post Office Box 30
State College, PA 16801

NAVY DEPARTMENT

NAVAL SEA SYSTEMS COMMAND

391 007

UNCLASSIFIED

SECURITY CLASSIFICATION OF THIS PAGE (When Data Entered)

REPORT DOCUMENTATION PAGE		READ INSTRUCTIONS BEFORE COMPLETING FORM
1. REPORT NUMBER TM 77-94	2. GOVT ACCESSION NO.	3. RECIPIENT'S CATALOG NUMBER
4. TITLE (and Subtitle) THE EFFECTS OF CLIPPING ON LINEAR BEAMFORMING WITH SINUSOIDAL INPUTS		5. TYPE OF REPORT & PERIOD COVERED M.S. Thesis, August 1977 6. PERFORMING ORG. REPORT NUMBER TM 77-94
7. AUTHOR(s) Arlen E. Breiholz		8. CONTRACT OR GRANT NUMBER(s) N00017-73-C-1418
9. PERFORMING ORGANIZATION NAME AND ADDRESS The Pennsylvania State University Applied Research Laboratory P. O. Box 30, State College, PA 16801		10. PROGRAM ELEMENT, PROJECT, TASK AREA & WORK UNIT NUMBERS
11. CONTROLLING OFFICE NAME AND ADDRESS Naval Sea Systems Command Department of the Navy Washington, D. C. 20362		12. REPORT DATE February 14, 1977 13. NUMBER OF PAGES 61 pages & figures
14. MONITORING AGENCY NAME & ADDRESS(if different from Controlling Office)		15. SECURITY CLASS. (of this report) Unclassified, Unlimited 15a. DECLASSIFICATION/DOWNGRADING SCHEDULE

16. DISTRIBUTION STATEMENT (of this Report)

Approved for public release, distribution unlimited, per NSSC (Naval Sea Systems Command), 5/11/77

17. DISTRIBUTION STATEMENT (of the abstract entered in Block 20, if different from Report)

18. SUPPLEMENTARY NOTES

19. KEY WORDS (Continue on reverse side if necessary and identify by block number)

transducers
arrays
clipping
signal processing

20. ABSTRACT (Continue on reverse side if necessary and identify by block number)

The problem addressed in this thesis is the overload of a linear transducer array. Under normal conditions, such overload results in clipping of the input signal. Such clipping may occur at the array elements or at the output of the beamformer with differing results. This paper presents a comparative study of the effect on beamformer performance of clipping at the transducer elements and of clipping at the beamformer output for sinusoidal signal and interference. The study was made using a computer simulation of a linear, → next page

DD FORM 1 JAN 73 1473 EDITION OF 1 NOV 65 IS OBSOLETE

UNCLASSIFIED

SECURITY CLASSIFICATION OF THIS PAGE (When Data Entered)

20. ABSTRACT (Continued)

single-line array connected to a bandpass spectrum analyzer. It was found that even hard clipping, i.e., clipping at a level far below that of the input signals, at the transducer elements had very little effect on the directivity of the array. Clipping at the output of the beamformer was found to have considerable effect on the directivity. This effect was strongly dependent upon the signal-to-interference ratio and upon the signal level at which clipping occurred. It was concluded that the beamformer should be designed so as to guarantee that if clipping is to occur, it be made to take place at the elements.

ACKNOWLEDGMENTS

The author wishes to express his sincere gratitude to Associate Professor Carter L. Ackerman for his guidance and advice. In addition, the advice of Dr. Paul H. Kurtz is gratefully acknowledged.

The research was supported by the Applied Research Laboratory of The Pennsylvania State University under contract with the U.S. Naval Sea Systems Command.

TABLE OF CONTENTS

LIST OF FIGURES

LIST OF FIGURES (Continued)

ABSTRACT

The problem addressed in this thesis is the overload of a linear beamformer. Under normal conditions, such overload results in clipping of the input signal. Such clipping may occur at the array elements or at the output of the beamformer with differing results. This paper presents a comparative study of the effect on beamformer performance of clipping at the transducer elements and of clipping at the beamformer output for sinusoidal signal and interference. The study was made using a computer simulation of a line array with a linear beamformer connected to a bandpass spectrum analyzer.

It was found that even hard clipping, i.e., clipping at a level far below that of the input signals, at the transducer elements had very little effect on the directivity of the line. Clipping at the output of the beamformer was found to have considerable effect on the directivity. This effect was strongly dependent upon the signal-to-interference ratio and upon the signal level at which clipping occurred. It was concluded that the beamformer should be designed so as to guarantee that if clipping is to occur, it be made to take place at the transducer elements.

CHAPTER I

INTRODUCTION

1.1 Brief Statement of the Problem

A practical array-beamformer combination presented with input signals sufficient to overload some portion of the network will produce nonlinear limiting, or clipping, in its output signal. Since the designer can control the dynamic range of each section of the network in order to place the clipping where he wills, it is desirable to know in which part of the network clipping causes the least degradation of directivity. The two locations most likely to minimize deterioration are: at the transducer elements (at the beamformer input) and at the output of the beamformer. The third alternative, which is to clip between multiplication of the inputs by the shading coefficients and the addition of the individual transducer element contributions, would negate the effect of shading. This will certainly affect the directivity strongly.

1.2 Scope and Limitations of the Present Study

This paper presents a comparative study of the effect on beamformer performance of clipping at the transducer elements and of clipping at the beamformer output for sinusoidal signal and interference. The study was made using a computer simulation of a line transducer array with a linear beamformer connected to a bandpass spectrum analyzer.

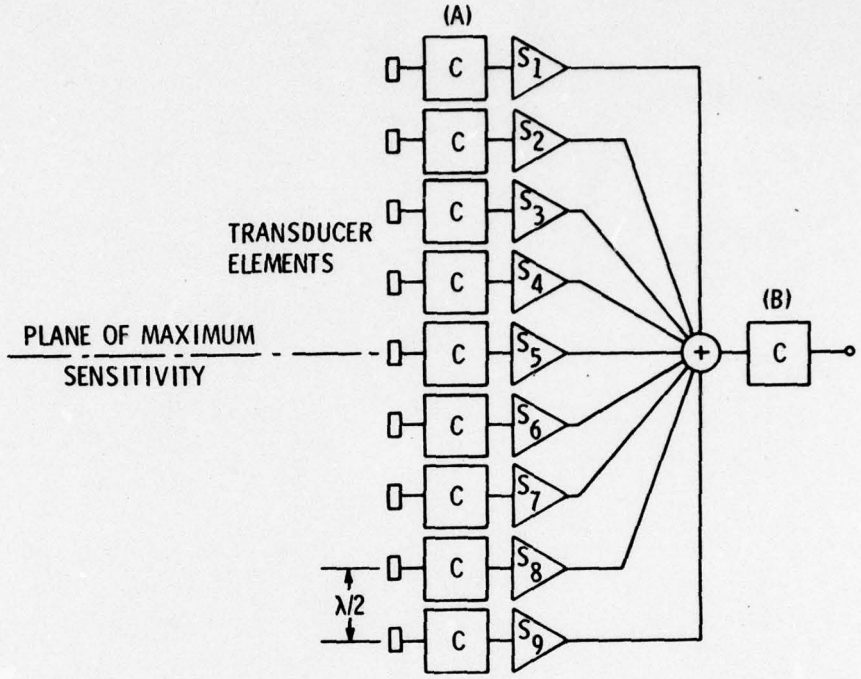

Figure 1.1 Diagram of a linear beamformer with a line array. The transducer elements are spaced at one-half of the operating wavelength. The boxes marked 'C' indicate the two optional clipping locations--before the beamformer (A) and after it (B). The scaling coefficients, S_n are chosen to give the desired interference rejection as a function of the interference angle measured from the plane of maximum sensitivity.

The voltage transfer function of the array-beamformer combination is

$$v_o(t) = \sum_{n=1}^{9} S_n v_s(t-r_n/c)$$

where v_s is the signal at the source, the r_n are the ranges from each element to the source, and c is the phase velocity of the lossless acoustic medium.

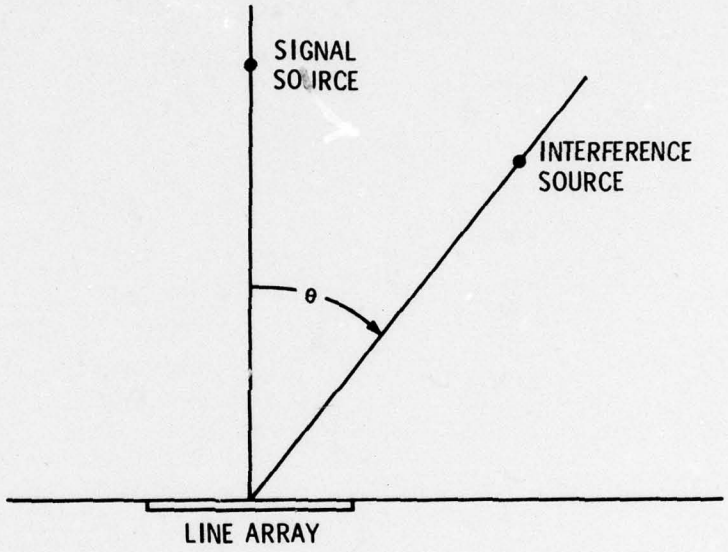

Figure 1.2 The definition of interference angle. The interference angle, θ, is the angle between the line from the center of the array to the interference source and the plane perpendicular to the line array.

It was found that even hard clippings, i.e., clipping at a level far below that of the input signals, at the transducer elements had very little effect on the directivity of the line array. Clipping at the output of the beamformer was found to have considerable effect on the directivity. This effect was strongly dependent upon the signal-to-interference ratio and upon the signal level at which clipping occurred. It was concluded that the beamformer should be designed so as to guarantee that if clipping is to occur, it be made to take place at the transducer elements.

CHAPTER II

NATURE OF THE PROBLEM

2.1 Phenomenon of Clipping

For purposes of this paper, we will distinguish between moderate clipping (Figure 2.1a) defined by the input-output relation:

$$V_{out} = \begin{cases} -AV_c & V_{in} < -V_c \\ V_{in} & -V_c < V_{in} < +V_c \\ +AV_c & +V_c < V_{in} \end{cases} \qquad (2.1)$$

and hard clipping (Figure 2.1b), in which

$$V_{out} = \begin{cases} -V_c & V_{in} < 0 \\ 0 & V_{in} = 0 \\ +V_c & 0 < V_{in} \end{cases} . \qquad (2.2)$$

At least for certain important cases, hard clipping is amenable to analytical investigation. The problem to be considered here is: what is the effect of clipping, especially moderate clipping, on the directivity of a linear transducer array? In particular, if clipping does occur, does it degrade the directivity of the line array-beamformer combination less if it occurs before the forming of beams or after?

This study made use of a computer simulation to answer this question for the case of a pulsed sinusoidal signal in the presence of an additive, sinusoidal interference. In this case, the degradation caused by clipping arises from the transfer of energy from

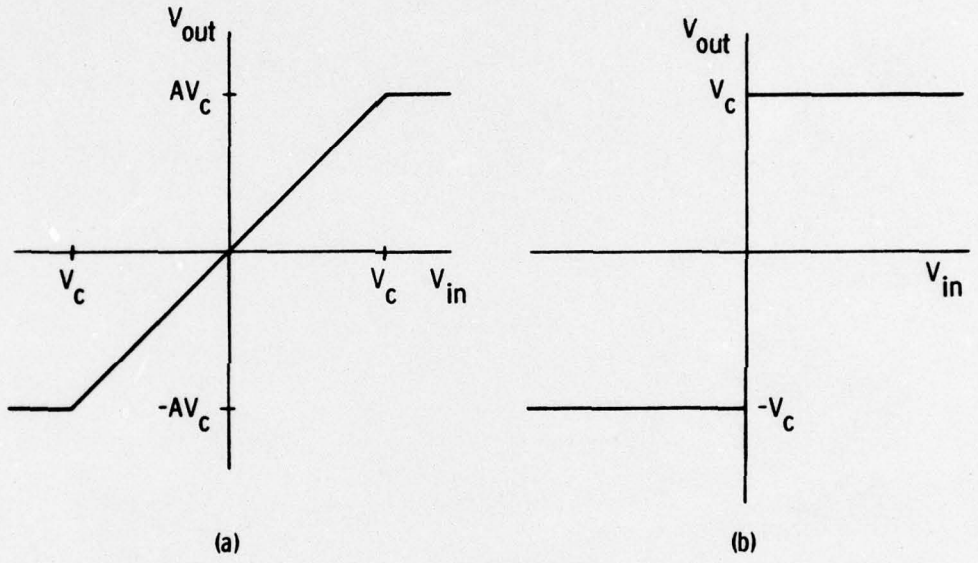

Figure 2.1 Voltage transfer characteristics of limiters defined in the text: a. A general clipped linear system. b. A hard clipper.

the input signal frequencies to frequencies which are harmonics of the input frequencies and "cross-products" of the input frequencies and their harmonics. An analysis of the response of a hard limiter to equal input signals is presented in the next section.

2.2 Analysis of the Frequency Distribution of Energy Under Hard Clipping

Consider two cosine functions of different frequency but equal amplitude,

$$f(t) = A\cos \omega_1 t \tag{2.3}$$

$$g(t) = A\cos \omega_2 t \ , \ \omega_1 > \omega_2 \ . \tag{2.4}$$

Adding these, we have

$$r(t) = A(\cos \omega_1 t + \cos \omega_2 t) \ . \tag{2.5}$$

If this sum is then transformed to a product by the appropriate trigonometric identity,

$$r(t) = 2A\{\cos\tfrac{1}{2}(\omega_1 + \omega_2)t\}\{\cos\tfrac{1}{2}(\omega_1 - \omega_2)t\} \ , \tag{2.6}$$

we see that the sum may be thought of as a cosinusoid at one-half the sum frequency modulated by another at one-half the difference frequency.

Hard limiting of this signal is equivalent to taking the signum function, r(t):

$$s(t) = \mathrm{sgn}[r(t)] = \mathrm{sgn}\{2A\cos\tfrac{1}{2}(\omega_1 + \omega_2)t \cos\tfrac{1}{2}(\omega_1 - \omega_2)t\} \tag{2.7}$$

$$= \mathrm{sgn}\{\cos\tfrac{1}{2}(\omega_1 + \omega_2)t \cos\tfrac{1}{2}(\omega_1 - \omega_2)t\} \ . \tag{2.8}$$

Since the value of the signum function depends only on the sign of its argument,

$$s(t) = \mathrm{sgn}\{\cos\tfrac{1}{2}(\omega_1 + \omega_2)t\}\,\mathrm{sgn}\{\cos\tfrac{1}{2}(\omega_1 - \omega_2)t\} \quad . \qquad (2.9)$$

This, however, is nothing more than a square wave at one-half the sum frequency modulated by another at one-half the difference frequency. These can then be expanded in Fourier series:

$$s(t) = \{\sum_{n=1}^{\infty} \frac{1}{2n-1} \cos \frac{2n-1}{2}(\omega_1 + \omega_2)t\}\{\sum_{m=1}^{\infty} \frac{1}{2m-1} \cos \frac{2m-1}{2}(\omega_1 - \omega_2)t\} \quad . \qquad (2.10)$$

This may be rewritten:

$$s(t) = \sum_{n=1}^{\infty}\sum_{m=1}^{\infty} \frac{1}{(2n-1)(2m-1)} \cos\{\frac{2n-1}{2}(\omega_1 + \omega_2)t\} \cos\{\frac{2m-1}{2}(\omega_1 - \omega_2)t\} \, . \qquad (2.11)$$

Now, returning to a sum-of-cosines form,

$$s(t) = \sum_{n=1}^{\infty}\sum_{m=1}^{\infty} \frac{1}{2(2n-1)(2m-1)}\{\cos\left|(n+m-1)\omega_1 + (n-m)\omega_2\right|t + \cos\left|(n-m)\omega_1 + (n+m-1)\omega_2\right|t\} \, . \qquad (2.12)$$

This is the simplest form of the result, but it is perhaps more instructive to put the result in the following form:

$$s(t) = \sum_{n=1}^{\infty}\sum_{m=1}^{\infty} \frac{1}{2(2n-1)(2m-1)} \left\{\cos\left\{\left|(2n-1)\frac{(\omega_1 + \omega_2)}{2} + (2m-1)\frac{(\omega_1 - \omega_2)}{2}\right|t\right\} + \cos\left\{\left|(2n-1)\frac{(\omega_1 + \omega_2)}{2} - (2m-1)\frac{(\omega_1 - \omega_2)}{2}\right|t\right\}\right\} \, . \qquad (2.13)$$

In this form, it is apparent that the additional frequencies, the cross-products, produced are not the sums and differences of the harmonics of ω_1 and ω_2 but are rather the sums and differences of the

odd harmonics of $\frac{1}{2}(\omega_1 + \omega_2)$ and $\frac{1}{2}(\omega_1 - \omega_2)$. All of these cross-product frequencies are present and the terms of the indices (p,q) where p and q are odd integers have amplitude $\frac{B}{2pq}$ where B is the clipping amplitude. Thus, for the case of equal signal and interference, it is possible to predict the frequencies and amplitudes of the cross-product components arising from the hard limiting process.

Now, consider the same analysis for two signals of amplitudes A and (A+a) where a > 0.

$$r(t) = A\cos\omega_1 t + (A+a)\cos\omega_2 t = A\{\cos\omega_1 t + \frac{A+a}{A}\cos\omega_2 t\} , \qquad (2.14)$$

but there is no trigonometric identity for this case comparable to the one used with equal signals. Let us try

$$r(t) = A(\cos\omega_1 t + \cos\omega_2 t) + a\cos\omega_2 t \qquad (2.15)$$

$$= 2A\{\cos\tfrac{1}{2}(\omega_1 + \omega_2)t\}\{\cos\tfrac{1}{2}(\omega_1 - \omega_2)t\} + a\cos\omega_2 t \quad . \qquad (2.16)$$

This corresponds to a modulated cosine (as in the equal-signal case) plus additional energy at one of the modulation sideband frequencies. If one attempts to clip r(t), the analysis fails because the signum function is nonlinear, i.e., the signum of a sum is not equal to the sum of the signums of the component functions.

It appears that no energy is present at frequencies other than those represented in the previous analysis, but the distribution of energy among those frequencies is unpredictable analytically. It is also evident that, if we consider hard clipping to be a limiting case of moderate clipping, the latter gives rise to energy only at the previously derived cross-product frequencies but again in unpredictable

proportions. Simulation therefore seems to be the expedient method of investigation with the case of hard-clipped equal signals offering a check on the accuracy of the simulation.

2.3 Structure of the Model System

Consider a communications system in which a single receiver is signalled by sixteen distinct sinusoidal sources. Each source is at a different frequency, and the receiver is to discriminate between the sources in spite of possible overload. Since the sources, although not fixed, are generally confined between two horizontal planes flanking the receiver, it is expedient to reject signals from above and below the receiver in order to reduce interference by reflections and sources not part of the communications network. To achieve this, a vertical line array transducer is used at the receiver. If it is assumed that although the signals from the source are of relatively long duration only the initial occurrence of the signal is of interest. Hence, once a signal has been detected it becomes interference to any subsequently activated signal. The necessary discrimination of sources and rejection of interfering sources can be achieved through the use of a matched filter for a sinusoidal signal.[1] This is easily implemented using fast Fourier transform techniques with a transform of sufficient size to allow easy frequency discrimination. A detailed description of a system of this sort suitable for the study of overload effects follows:

---

[1] L. A. Wainstein and V. D. Zubakov, Extraction of Signals from Noise, translated from Russian by Richard A. Silverman (Englewood Cliffs, N.J.:Prentice-Hall, Inc., 1962), pp. 80-117.

The simulation program used for this study is based on a hybrid analog-digital-receiver as shown in Figure 2.2. The input to this receiver comes through a line array of nine identical transducer elements. The spacing between the elements is one-half of the wavelength of the center frequency of the detection band. The output signals from the transducers are weighted by appropriate amplitude shading coefficients and added to form a highly direction beam in the plane of the line array.

The output of this beamforming circuitry is passed through an analog bandpass filter. This filter prevents the aliasing, or folding back, of extraneous signal component frequencies into the analysis band in the sampling process.

The filter is followed immediately by a sampler which forms quadrature sample pairs at (or above) the Nyquist rate for the band-limited signal. A complex array of 128 consecutive quadrature pairs is formed. This array is passed to a bandpass spectrum analyzer which is implemented by computing the fast Fourier transform (FFT) of this array.

The output spectrum, which is also a complex array, is converted to a magnitude spectrum by multiplying each array element by its complex conjugate and extracting the square root of this real number. Before the arrival of the signal, this spectrum is considered to be a "background" spectrum. The magnitude spectrum is then smoothed by averaging groups of five adjacent array elements and assigning this average value to the central element of each group. (The two points at either end are assigned the same value as the third

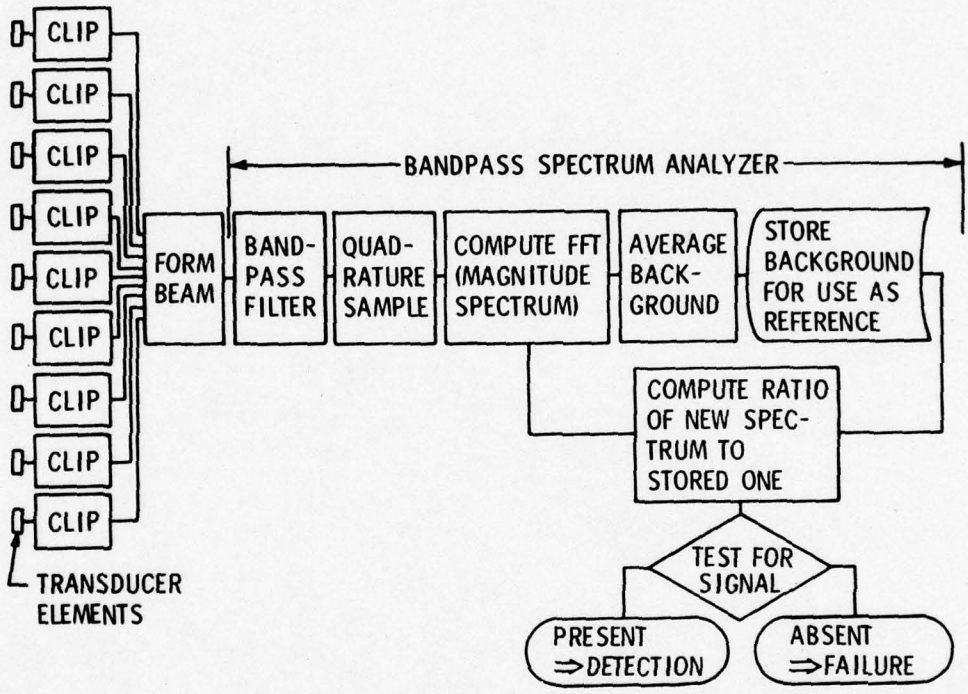

Figure 2.2 Block diagram of the model receiver on which the simulation program was based.

point from their respective ends.) This averaged spectrum is stored for comparison with the next spectrum to be taken.

When a pulse has been transmitted, the received magnitude spectrum is compared to the averaged background spectrum by dividing each element of the new spectrum array by the corresponding element of the averaged background spectrum. The ratio is expressed in decibels for convenience. This ratio, or difference, spectrum is then scanned for values greater than some threshold level. If there is a threshold crossing, the largest value in the ratio spectrum is taken as the desired signal.

2.4 Structure of the Simulation Program

The simulation program (Figure 2.3) for this system differs from the model system in that samples must be formed immediately, and all processes must then be performed on the sampled data. After the input parameters needed by the program are read, the element and source positions are computed. The element positions are computed as the half-wavelength of the interference rather than the center frequency of the band in order to eliminate some superfluous harmonics of small magnitude. The distance and the corresponding time delay between each source and each element is then computed. The time delays are normalized by subtracting the delay between a source and one element, so that only the relative delays between elements for each source are retained. Samples of the signal and interference sine waves are then generated with phase terms corresponding to the time delays for each element. These samples are clipped, after which they are weighted by the shading coefficients

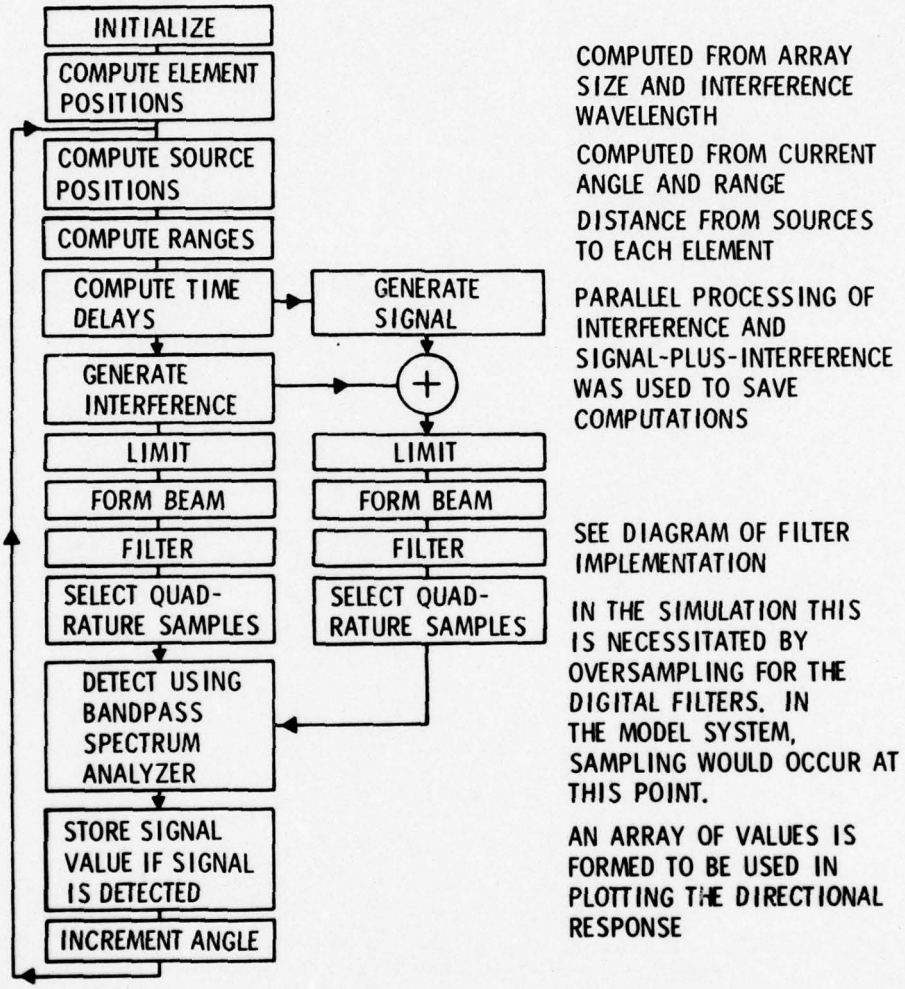

Figure 2.3 Flow diagram of the simulation program.

and summed to form beams. For tests of clipping after beamforming, the clipping is placed after the summation.

The beamformer outputs are then filtered to remove harmonics generated by the clipping process. It is at this point that the simulation becomes radically different from the hybrid system. Where a relatively simple analog bandpass filter is sufficient in the hybrid system, the aliasing phenomenon necessitates a three-stage cascade of digital filters using samples taken at a rate at least three orders of magnitude greater than the Nyquist rate. (For a complete discussion of the filter problem, see Section 3.4.) Quadrature sample pairs are chosen at the Nyquist rate from the filter output and stored in a complex array.

This array is passed to an FFT subprogram just as it would be in the hybrid system. The spectrum analyzer is the implemented as it was in the hybrid model.

Three major problems arose in the implementation of the simulation. One of these, error in the approximation of the Hilbert transform by quadrature samples, is inherent in the model hybrid system as well as in the digital simulation. The other two, beamforming error and simulation of an analog filter by a digital one, arise from limitations imposed by the generation of samples immediately rather than after analog processing. These three problems and the implementation of the bandpass spectrum analyzer are discussed in detail in the next chapter.

CHAPTER III

DETAILS OF THE SIMULATION

3.1 Implementation of the Bandpass Spectrum Analyzer

Two fast Fourier transforms are required to perform the signal detection process. The first is taken before the signal is received and contains only the interference signal. This transform acts as a reference, or "background" spectrum. The complex array output by the FFT subprogram is converted to a real magnitude array by computing the square root of the sum of the squares of the real and imaginary parts of each of its elements. It then undergoes a sliding average in which each group of five adjacent points is averaged. This averaged array is then stored until a new set of data with the desired signal included is collected and processed by the FFT. Each element of this new array is then divided by the corresponding entry of the averaged reference array, and the ratio is expressed in decibels. This ratio (or, in terms of decibels, difference) array is then searched for values above the threshold level. If a single entry exceeds the threshold level, it is taken to be the desired signal.

When no clipping occurs, the first of the two FFT spectra (Figures 3.1, 3.2) contains a single peak at the interference frequency. The second spectrum (Figure 3.3) contains a peak at the interference frequency and an additional peak at the signal frequency. The ratio spectrum (Figure 3.4) displays a high signal peak, but the interference

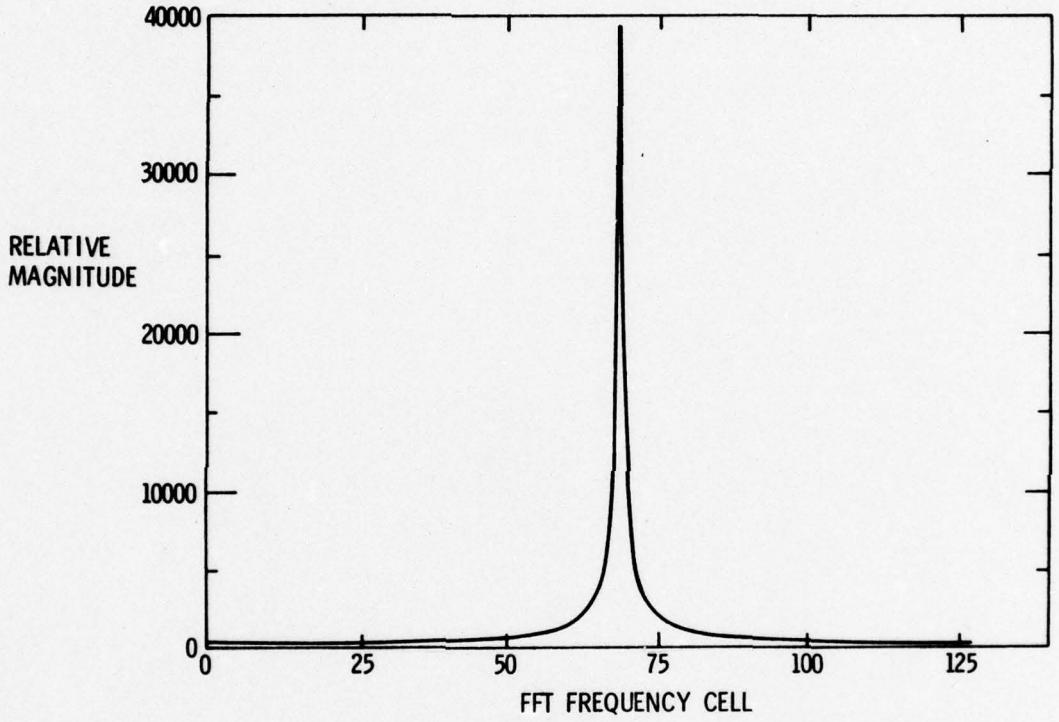

Figure 3.1 Magnitude spectrum of the interference-only (background plot). The interference is unclipped.

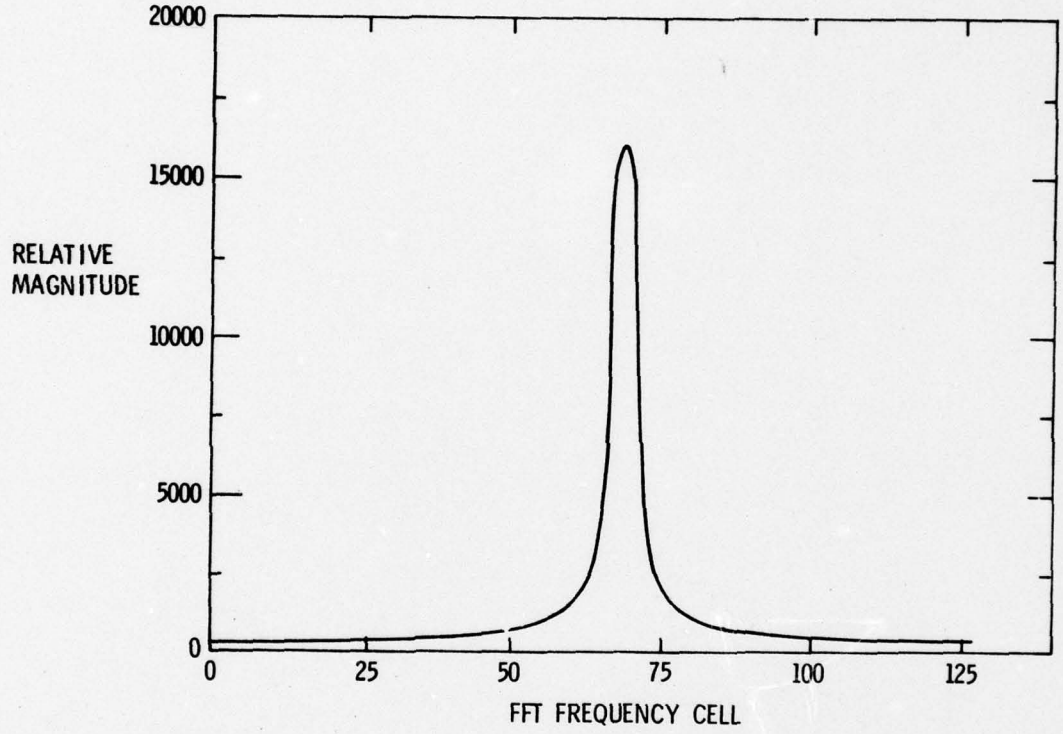

Figure 3.2 Averaged background magnitude spectrum. The background plot of Figure 3.1 averaged by the sliding window averaging routine. Groups of five cells are averaged.

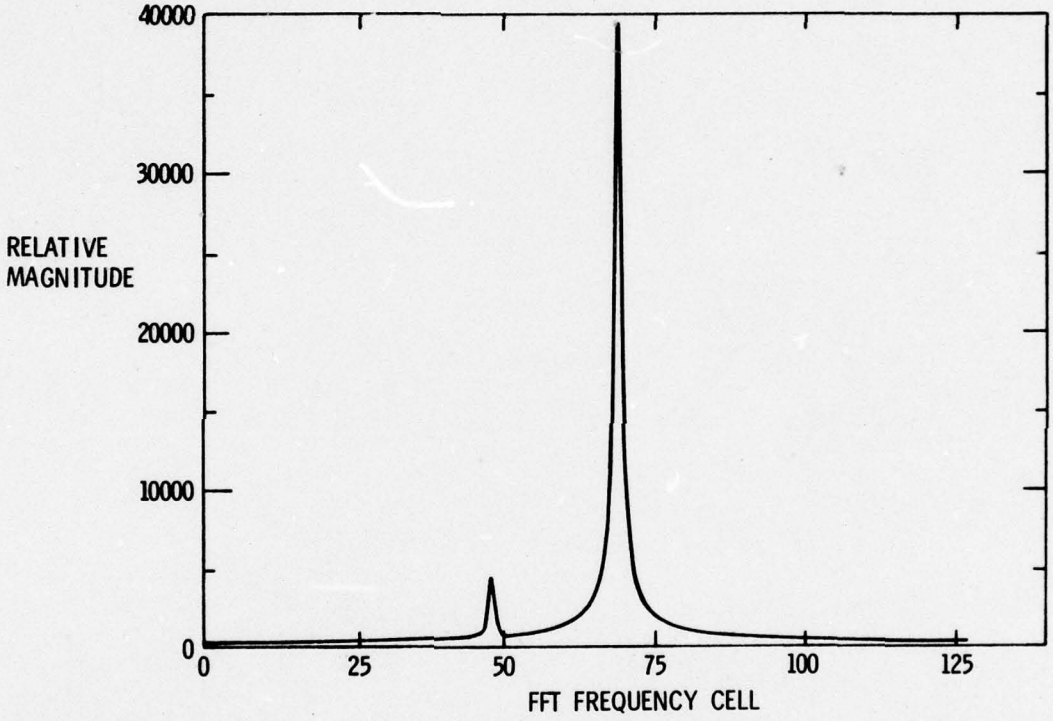

Figure 3.3 Magnitude spectrum of the unclipped signal-plus-interference. The signal is 20 dB below the interference. Neither is clipped.

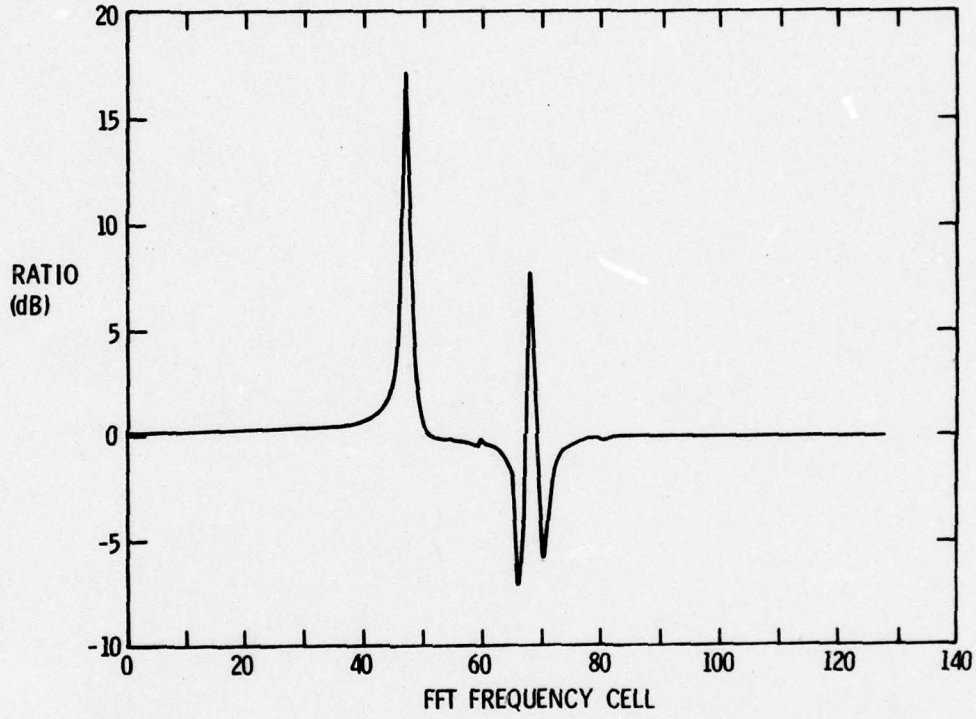

Figure 3.4 The magnitude ratio spectrum of the case shown in Figures 3.1-3.3. The signal is 20 dB below the interference, and neither is clipped. Note the quadrature error peak in cell 60 due to the interference signal.

peak is suppressed because the background magnitude is large at that frequency.

When clipping takes place, the first spectrum remains basically unchanged in appearance (though not necessarily in magnitude) because the filter suppresses the harmonics of the interference frequency. The second spectrum, however, is corrupted by cross-products of the signal and the interference (Figure 3.5). The levels of some of these cross-products in the ratio spectrum (Figure 3.6) are nearly as large as the level of the signal peak. It is possible that one of these spurious peaks might be falsely detected as the signal. This would happen if the first spectrum happened to be substantially higher at the signal frequency than at the cross-product frequency. This is possible if the signal frequency is very close to the interference frequency. In practice, this problem might be overcome by a more elaborate detection algorithm. Such an algorithm might make use of the absolute signal magnitudes from the second FFT spectrum or of a priori knowledge of the approximate signal location.

The algorithm as described above proved quite adequate for use in simulation in which the signal and interference frequencies were under the user's control. The program which was used followed this detection scheme exactly except that the interference and the signal-plus-interference data were processed in parallel to avoid redundant computation (Figure 2.3).

3.2 Effects of Quadrature Sampling

It is mathematically possible to eliminate the negative frequency components from the Fourier transformation of a real signal by

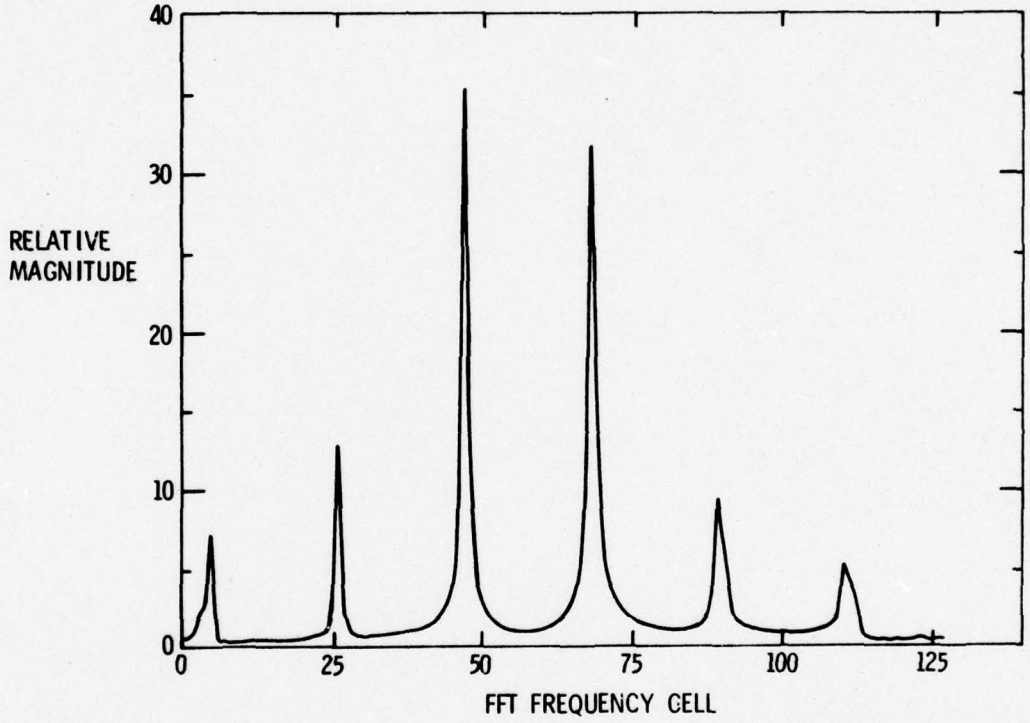

Figure 3.5 The magnitude spectrum of hard-clipped, equal signals on axis. The pairs of peaks are due, in descending order of height, to the first, third, and fifth harmonics of one-half the difference of the input frequencies.

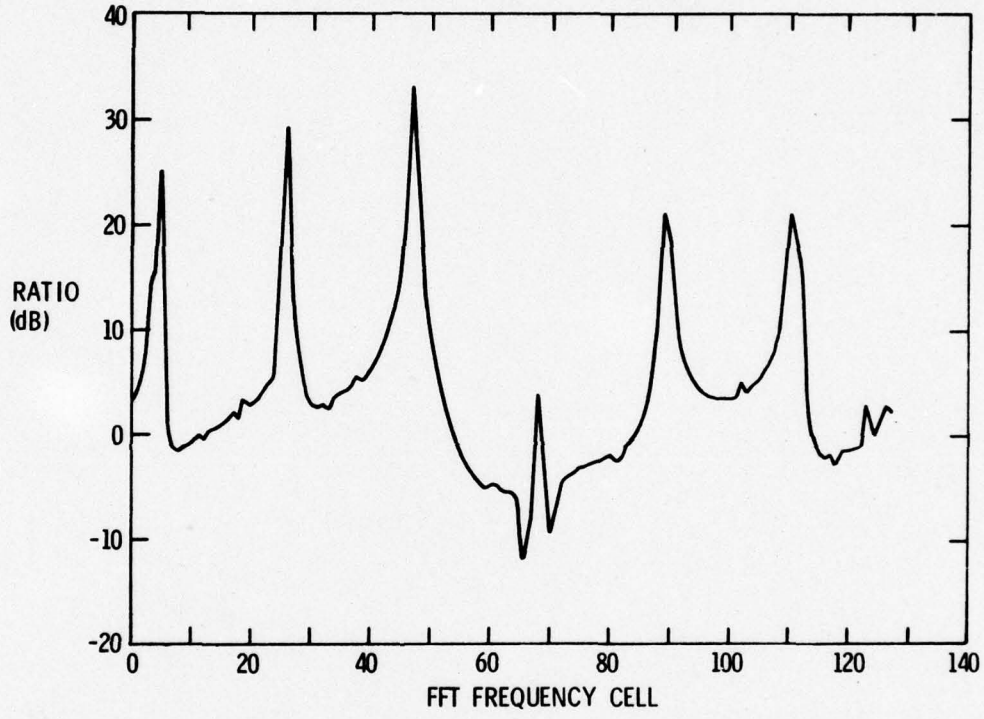

Figure 3.6 The ratio spectrum of hard-clipped, equal signals on-axis. The minor peaks at 60 and 80 are due to quadrature error of the signal and interference. Other small peaks are error on cross-product terms and higher order cross-products not totally eliminated by the digital filter.

transforming not the signal alone, but its pre-envelope. The pre-envelope of a signal is a complex signal whose real part is the signal and whose imaginary part is the Hilbert transform of the signal. The Hilbert transform is defined as:

$$\overset{\Lambda}{x}(t) = \frac{1}{\pi} \int_{-\infty}^{\infty} \frac{x(u)}{t-u}\, du \quad , \tag{3.1}$$

where the notation $\int$ indicates the Cauchy principal value of the integral. Thus, the pre-envelope of signal, $x(t)$, with Hilbert transform, $\overset{\Lambda}{x}(t)$, is:

$$s(t) = x(t) + j\, \overset{\Lambda}{x}(t) \quad . \tag{3.2}$$

The Fourier transform of the pre-envelope of a real signal has only positive frequency components, and their magnitude is twice that for a two-sided spectrum.

For a narrow-band, sampled signal, it is possible to form an approximate pre-envelope which suppresses negative frequency components in the FFT spectrum. The technique used is based on the fact that the cosine function is the Hilbert transform of the sine function. If a narrow-band signal is delayed one-quarter period of some frequency within the band (usually the center frequency), the undelayed signal may be taken as an approximation to the Hilbert transform of the delayed signal. These two signals could then be sampled simultaneously and the samples used to form an approximation to the sampled pre-envelope, $s(t)$. The analog time delay can be removed by taking the pairs of samples separated by one-quarter of the period of the quadrature center frequency, i.e., that frequency for which the quadrature sampling is

to give an exact pre-envelope. As long as the signals to be sampled are limited to a band very narrow relative to its center frequency, the error committed in using this quadrature sampling approximation to the pre-envelope is small.

The error in quadrature sampling manifests itself in the appearance of energy at the negative frequency corresponding to each positive frequency component of the signal. The aliasing phenomenon causes this error energy to appear in discrete Fourier transform spectra of the signal as spurious peaks. For each positive frequency peak there will be a small (for narrow-band signals) negative frequency peak at the reflection of the positive frequency location across the quadrature-sampling center frequency.

Consider the effect of violation of the narrow-band restriction. For example, if the quadrature sampler is presented with a signal at twice the quadrature center frequency, the effective quadrature delay is one-half period, and there is effectively no quadrature sampling. That is, the positive and negative frequency components are equal. If the signal to be sampled is at three times the quadrature center frequency, the effective quadrature delay is three-quarters of a period which corresponds to minus one-quarter period. In terms of the Hilbert transforms of sinusoids, this is effectively the negative of the Hilbert transform giving a pre-envelope,

$$s(t) = x(t) - j\,\hat{x}(t) \quad . \tag{3.3}$$

This results in the suppression of the positive spectrum and the doubling of the negative components. In general, even harmonics of

the quadrature center frequency produce equal positive- and negative-frequency components. The harmonics given by the sequence 1,5,9,13,... produce only positive-frequency components. The remaining harmonics produce only negative-frequency components. Signals which are not harmonics of the quadrature center frequency produce both positive- and negative-frequency components whose relative size depends on whether the frequency of the signal is closer to an odd harmonic having a positive-frequency image or to one with a negative-frequency image.

In the simulation, the bandpass filter serves to eliminate frequencies sufficiently far from the quadrature center frequency that they have large negative frequency components when quadrature sampled. The error consists only of small peaks which are identifiable as arising from quadrature error and which are not sufficiently large to interfere with detection.

3.3 Simulation of Beamforming

The fundamental consideration in the digital simulation of analog beamforming was the accuracy with which the fundamental operations could be carried out. The accuracy of an analog beamformer is limited by the tolerances of its components and the placement of the transducers and by its self-noise. The digital simulation is limited by the length of its number representation. It was found that a much lower noise level could be attained through the use of double-precision (8 byte) real number representations in the section of the program from the generation of the samples through the completion of beamforming. The improvement in accuracy is most notable for hard clipped signals

whose zero-crossings are not as well defined in single precision as they are in double precision. This gives rise to jitter in the apparent zero-crossing locations which appears as high-frequency noise in the frequency spectrum.

Beamforming in single precision also suffers from the accuracy problem associated with subtraction whose difference is orders of magnitude smaller than its terms. This effect, like the other, is more pronounced when the interference source is off the axis of the beam where cancellation is strong so that the beamformer output is at a much lower level than its inputs.

3.4 Simulation of an Analog Filter by a Digital Filter

The most difficult problem of the simulation was the development of a suitable model for the analog bandpass filter. This filter is needed to suppress the harmonics generated by the limiter, so that they will not fold back into the analysis band of the spectrum analyzer and interfere with detection. Hard limiting gives rise to square waves as input signals. These have Fourier coefficients whose magnitudes are proportional to the reciprocal of their (odd) order. That is, the signal includes the fundamental, a third harmonic of one-third the amplitude of the fundamental, a fifth harmonic of one-fifth the amplitude of the fundamental, and so on. Since these harmonics are relatively large, even at high orders, it is necessary to have an effective filtering system if they are not to interfere with detection.

The first approach taken to the problem of harmonic suppression was the use of an elliptic filter. This operated on quadrature sample pairs taken at twelve times the FFT sample rate, the appropriate

samples being selected at the output of the filter. The zeros of this filter were chosen to cancel the first few harmonics of the input frequencies. This filter had the disadvantage of restricting the useable test frequencies to those whose harmonics must be suppressed to provide relatively "clean" FFT spectra. Without a filter, the ninth harmonic was only 19 dB below the fundamental, and the ninety-ninth harmonic was only 40 dB down. It was decided that all harmonics out to the ninety-ninth should be suppressed.

This suppression was accomplished through the use of a multi-stage cascade of digital filters operating at successively lower sampling rates (decimation in time) as shown in Figure 3.7. To achieve the desired goal, evenly spaced samples were generated at a rate 1350 times the desired sample rate for the spectrum analyzer. Clipping and beamforming were done at this rate, and the resultant waveform was passed through a two-pole digital Butterworth lowpass filter with a half-power frequency slightly above the final desired band edge (Figure 3.8, solid line). This filter attenuated the highest harmonics of interest sufficiently that it was possible to subsample by a factor of five, that is to retain only every fifth sample coming out of the filter. This was advantageous since only two poles of the complete filter were computed at the highest rate, and subsequent filter sections could be computed for far fewer samples.

The samples retained in the subsampling process were passed to a four-pole Butterworth lowpass filter (Figure 3.8, dotted line) which removed enough additional harmonics to allow subsampling by a factor of five again.

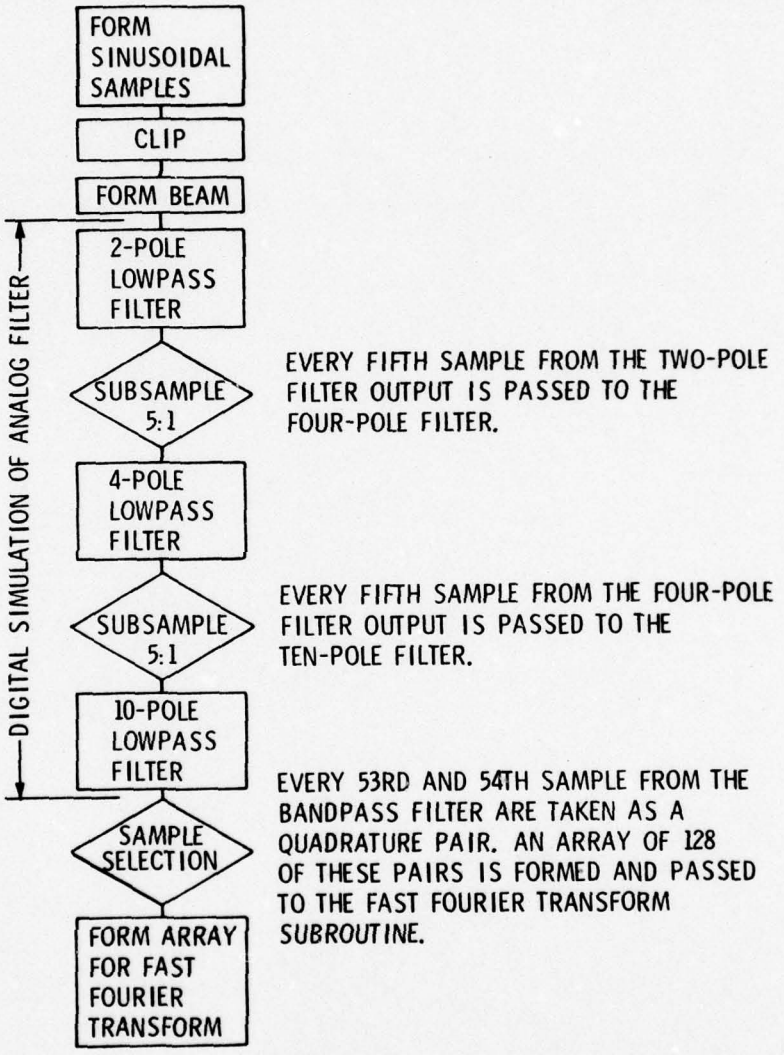

Figure 3.7 Flow diagram of digital filter simulation of the analog filter.

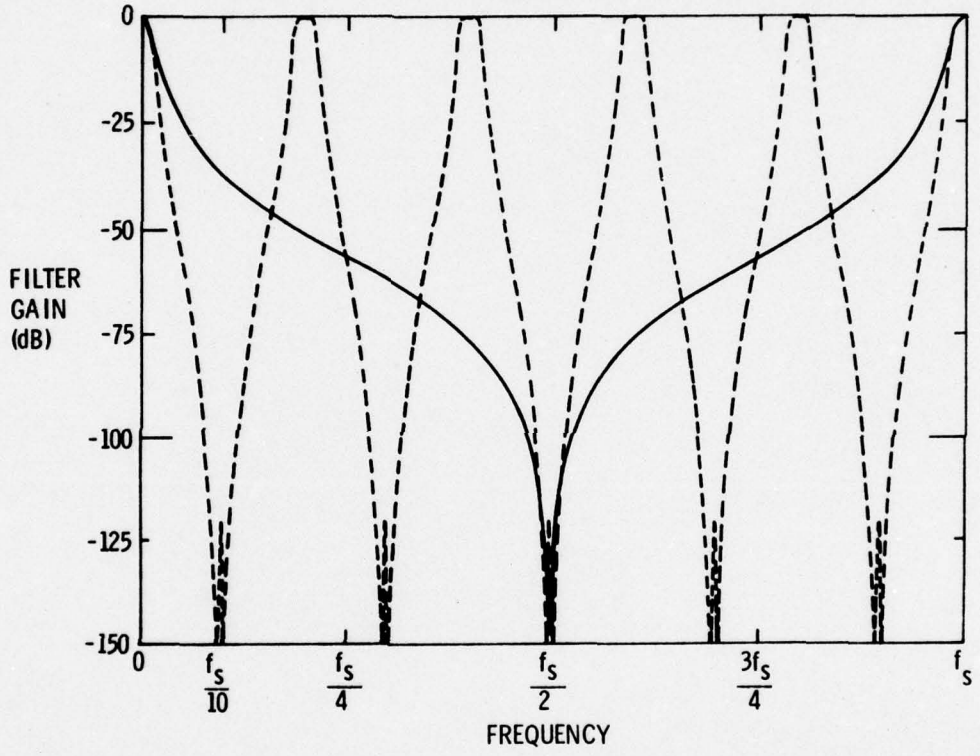

Figure 3.8 Frequency response of the two-pole Butterworth lowpass filter (solid line) and the four-pole Butterworth lowpass filter (dotted line). f_s is the initial sampling frequency.

These samples, now at one twenty-fifth the original rate were filtered by a ten-pole Butterworth bandpass filter with half-power frequencies slightly outside the analysis bands (Figures 3.9, 3.10). The output of this filter was subsampled by a factor of fifty-four to reach the Nyquist rate for the desired analysis band. Since the sample period at the output of the bandpass filter was equal to the desired quadrature delay, adjacent pairs of samples were taken as quadrature sample pairs of the final subsampling rate.

This cascade of filters with decimation in time effectively removed all harmonics as well as strongly attenuating out-of-band cross-products resulting from the clipping of the sum of two sinusoids.

Since any filter would have to operate at 1350 times the final sample rate in order to suppress the ninety-ninth harmonic, the cascade required substantially fewer computations than the direct implementation. Only two poles of the cascade were computed at the highest rate and four at the second highest rate. The large ten-pole section needed to process only one twenty-fifth of the samples generated. This offered considerable savings over a direct implementation in which eight or more poles must process samples at the high rate. This time factor was significant since the quantity of multiplications necessary is quite large. It was found that even with the use of trigonometric identities to move subprogram calls and function computations outside the inner loops of the program, more than ten minutes were required to complete the entire sample generation and detection process for one interference angle on a computer with an 8.5 ms. double-precision multiplication time. Thus, a polar plot with two-degree resolutions took about nine hours.

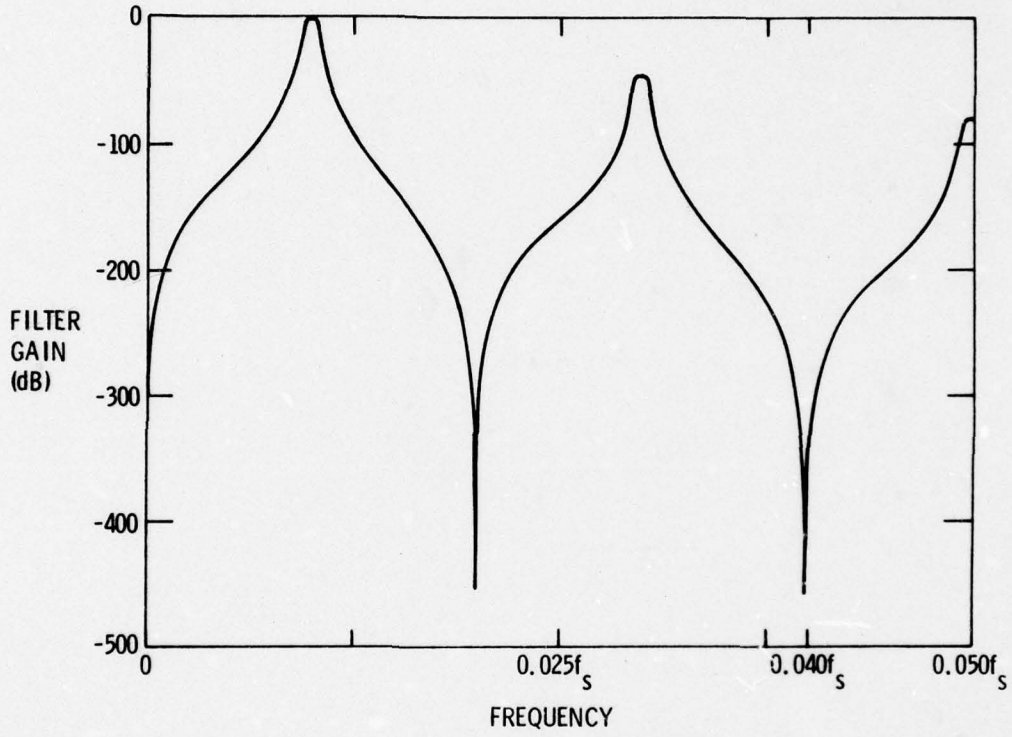

Figure 3.9 Frequency response of the cascade of three digital filters in the region of the passband. f_s is the initial sampling frequency; $0.04f_s$ is the sampling frequency for the bandpass filter.

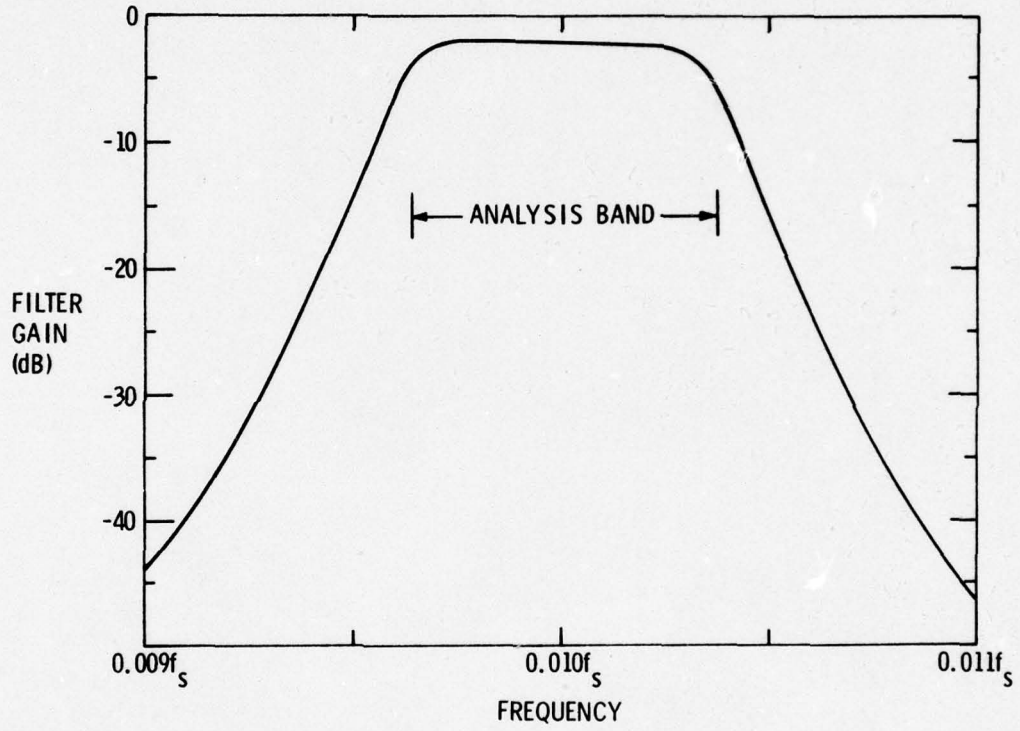

Figure 3.10 Frequency response of the cascade of digital filters in the passband. The analysis band of the fast Fourier transform is indicated.

CHAPTER IV

RESULTS OF THE SIMULATION

4.1 Effect of Hard Clipping at the Transducer Elements

The discussion in this and the following sections refers to Figures 4.1 and 4.4-4.9 which are plots of the rejection of the interference as a function of the interference angle as defined in Figure 1.2. The angles for which these data are plotted are from -90° to 0° in 2° increments. This range is sufficient since the curves are symmetric about zero degrees.

As can be seen in Figure 4.1, the effect of hard clipping at the transducers on the directional response of the line is relatively minor. Although the clipped case is not as smooth as the unclipped case, the sidelobes remain more than 40 dB below the main lobe. The fluctuations in response in the region of high attenuation at large angles probably arise from the transfer of energy between the signal and harmonic and cross-product frequencies as the beamformer creates output waveforms rich in harmonics. (Figure 4.2 shows the time waveform at the beamformer output for such a hard-clipped case.) The deterioration of the deep nulls in the response is reasonable since it is the almost perfect cancellation of sinusoidal signals in the unclipped case which creates these nulls. The square waves of the hard-clipped case simply do not cancel as well as the sine waves for which the line was designed.

The frequency spectra show cross-product frequency components as expected (Figures 3.5, 3.6). Those cross-products arising from

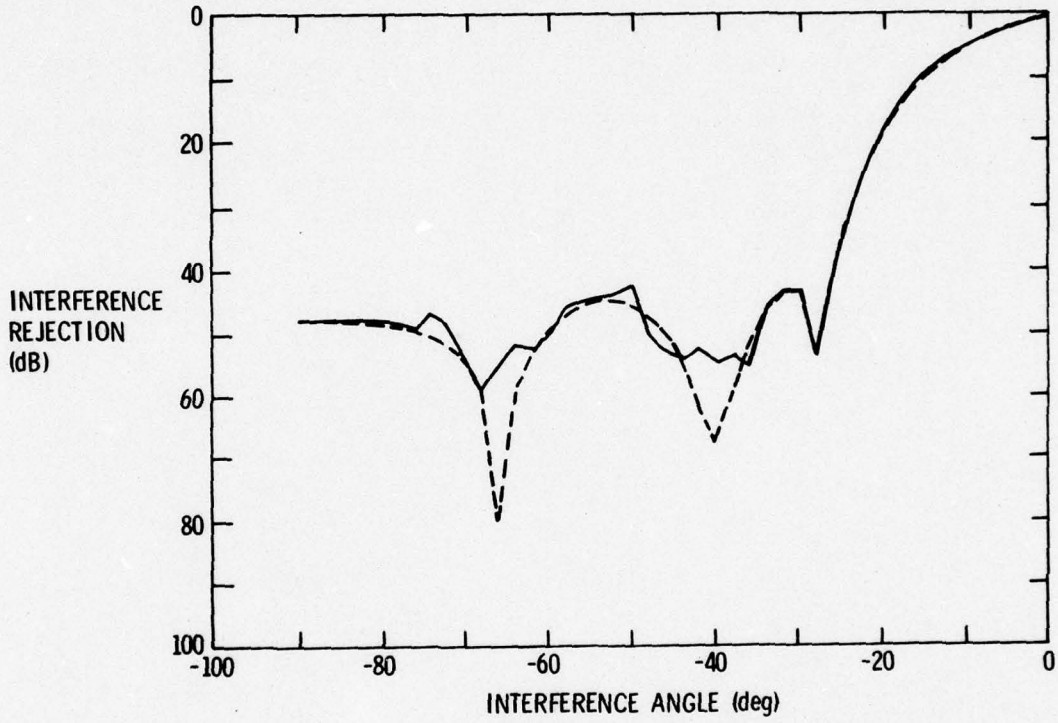

Figure 4.1 Directivity of the array under hard limiting. Solid: Clipped 60 dB below the interference level. Dotted: Unclipped. Signal 20 db below interference in each case.

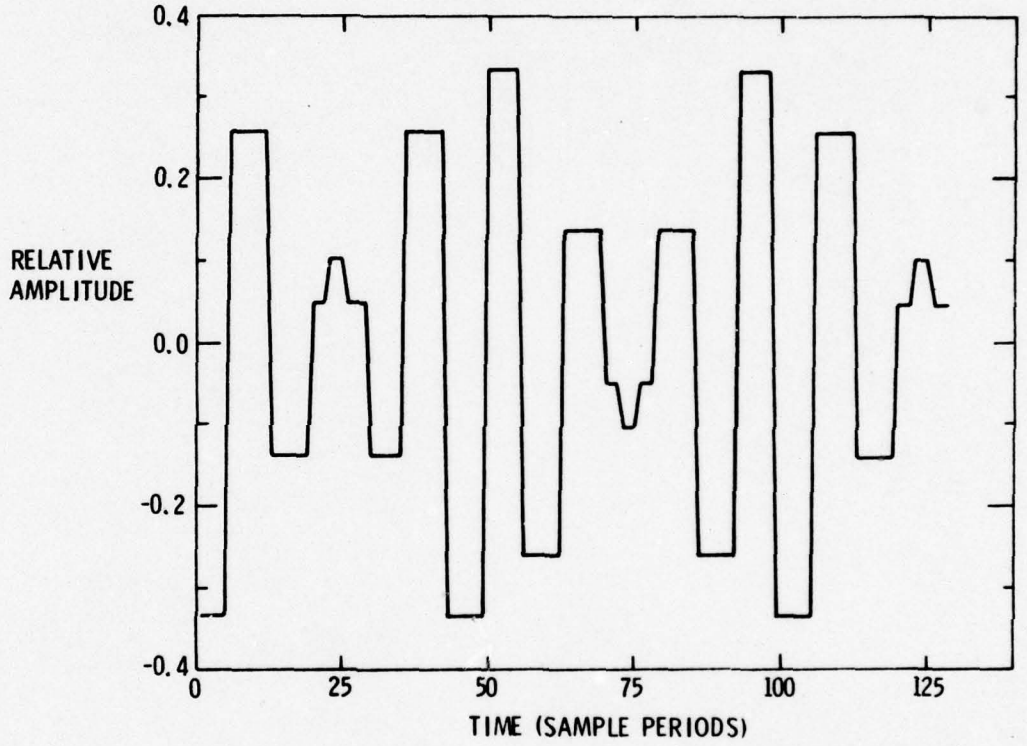

Figure 4.2 Waveform at the output of the beamformer for hard-clipped signal-plus-interference, the signal 20 dB below the interference, at an interference angle of 60°.

the third and fifth harmonics of one-half the difference frequency are in the analysis band and are quite strong. Images of the out-of-band seventh harmonics are also aliased into the band. These are highly attenuated by the filter, however, and are therefore of little interest. Although they are not of sufficient strength to interfere with the detection process for the frequencies used in preparing this report, it is possible that one of these peaks might exceed the desired signal for some combinations of frequencies. This might result in failure to detect a signal. Perhaps it is more likely that the highest cross-product will be chosen as the signal. Although this is an error condition, it does correctly determine that some source is present although its frequency is incorrectly determined. Additional minor peaks seen in the spectrum analyzer output correspond to quadrature sampling error images. These and the in-band cross-products would be present in the hybrid system. The out-of-band cross-products might be more strongly attenuated by an analog filter although they would probably still be present.

As the interference source is moved off the peak response direction, the cross-product components are attenuated along with the interference (Figure 4.3). This is to be expected since the phase of each cross-product term at each element is a combination of the phase of the signal and the phase of the interference. Since the signal source does not move, its phase shift at each element is constant. The phase of the interference, which changes as the source moves, controls the phase of the cross-products at the individual elements. Hence, the cross-products are attenuated by the beamformer along with the interference.

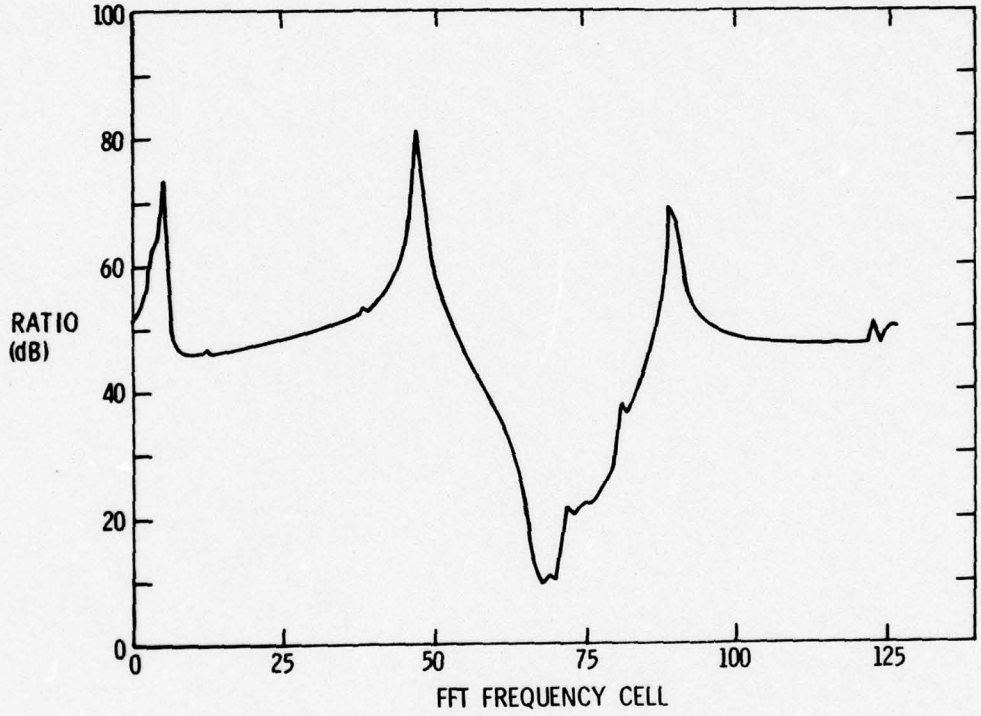

Figure 4.3 The ratio spectrum for hard-clipped, equal signals with the interference 90° off the array axis. Compare to Figure 3.6 to see the effects of the array on the cross-product magnitudes.

The relationship of the amplitudes of the various cross-products is not constant as the angle of the interference source changes. This is because of the complexity of the waveform created by the beamformer (Figure 4.2). As the angle changes, energy is shifted into different harmonics and cross-product frequencies as the beamformer output wave shape changes. Fortunately, the ratios of the magnitudes of the interference and signal peaks to their respective side-lobe magnitudes deviate by no more than a few decibels from the unclipped case throughout the range of interference angles. Thus, the directional response of the hard-clipped case is acceptably close to that of the unclipped case despite its noisiness.

4.2 Effect of Moderate Clipping at the Transducer Elements

As might be expected from examination of the results for hard limiting, moderate clipping has little effect on the directional response of the simulation. Figure 4.4 shows the interference rejection of the system clipped at 70.7% of the peak interference amplitude plotted together with the response in the unclipped case. In this case, only one of the response notches is affected, and the response curve is somewhat smoother than in the hard-clipped case. Those effects which do manifest themselves are as discussed previously for the hard-clipped case (Section 4.1). The plots produced by the spectrum analyzer again display cross-product peaks of considerable magnitude, although there are fewer peaks present. It appears that clipping to a degree which might be expected in a moderate overload situation can be tolerated quite well by the system simulated here.

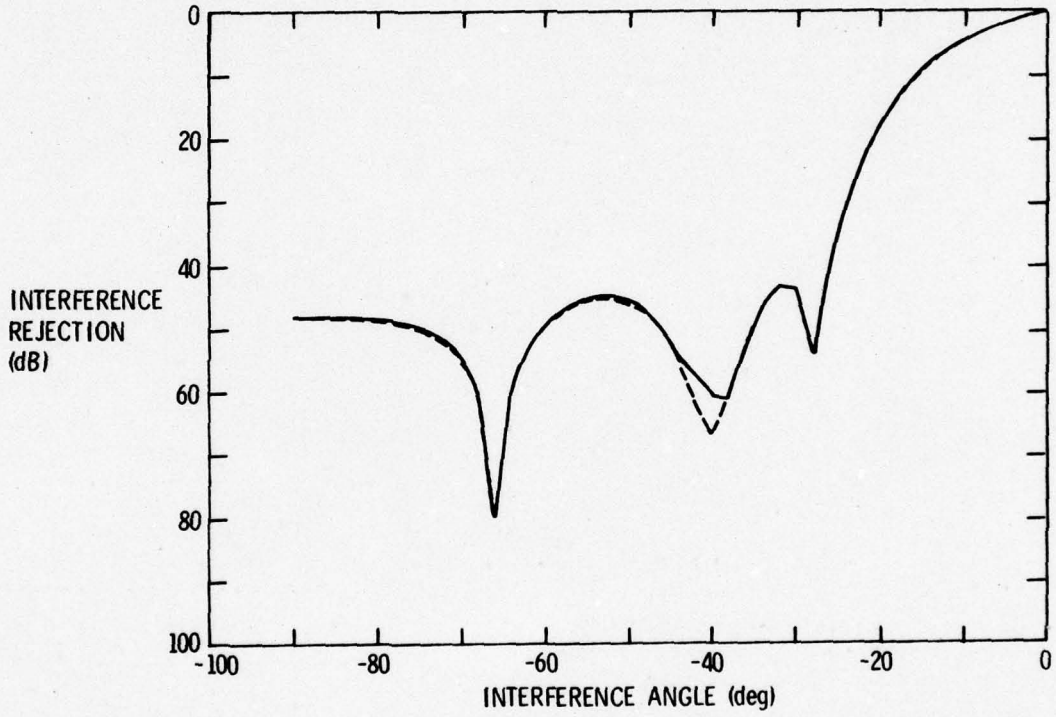

Figure 4.4 Directivity of the array under moderate limiting. Solid: Clipped at 3 dB below interference level, signal 20 dB below interference. Dotted: Unclipped.

4.3 Effect of Decreased Signal-to-Interference Ratio

The case of hard clipping was tested twice. In the first instance, a 0 dB signal-to-interference ratio was used, and in the second, a -20 dB ratio was tested. The directivity patterns generated in these tests are plotted together in Figure 4.5. For most angles, the difference in the two curves is negligible. The only significant difference is the slight flattening of the main lobe in the -20 dB signal-to-interference ratio case. Since the background spectra of the two cases are identical, the effect must be due to some variation in the signal level in the signal-plus-interference spectrum. The limiter is a device whose output power is approximately constant as long as limiting is occurring. If two signals of different frequency are limited, the resultant waveform will include power at each of those signal frequencies (and others as well, see Section 2.2). If one signal is much larger than the other, it will dominate the output. However, as the relative amplitude of the smaller signal is increased, the percentage of the output power at its frequency will also increase (the total output power always remaining constant). Finally, a transition region occurs in which the signals are approximately equal so that neither dominates. Because of the nonlinearity of the limiting process, the rate of growth of the component at the signal frequency varies with signal-to-interference ratio, particularly between the small-signal and transition regions.

These normalizing effects occur as the interference source moves out of the plane of maximum response allowing the output at the signal frequency to become larger. In the equal-signal case, the process starts in the transition region, but in the unequal signals case the

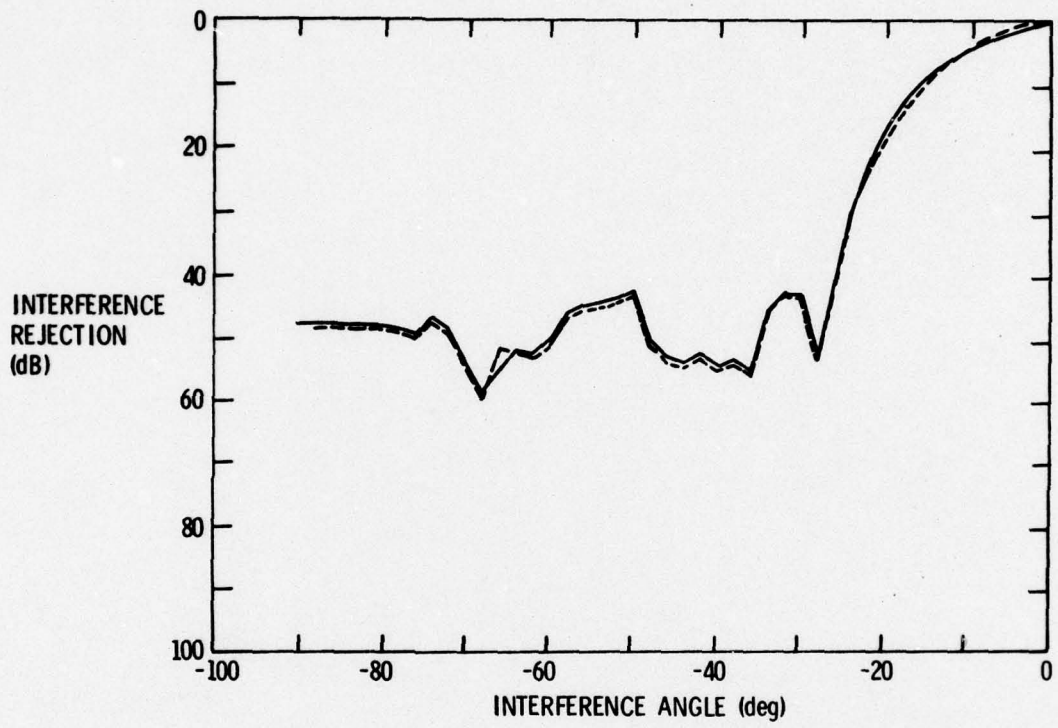

Figure 4.5 Variation of directivity with signal-to-interference ratio under hard clipping. Solid: Signal 20 dB below interference. Dotted: Signal equal to interference. Both are clipped 60 dB below the interference level.

interference dominates near the plane of maximum response. The non-linearity of the signal growth causes the relative growth of the signal with movement of the interference off-axis to depend on the on-axis signal-to-interference ratio. Hence, the transfer of energy between the two signals in the transition region does not proceed at the same rates as that between grossly unequal signals. This slight discrepancy is seen as an apparent flattening of the main lobe of the unequal-signals response. That is, the interference is being attenuated more rapidly near the axis in the unequal-signals case then it is with equal signals. Fortunately, the effect is a minor one and has only the small effects shown in Figure 4.5 on the directivity pattern.

The system appears to perform reliably for those signal-to-interference ratios for which detection is possible with the exception of possible cases in which a cross-product is erroneously detected as described in Section 3.1. The determination of the minimum detectable signal-to-interference ratio for such cases was not within the scope of this study. It was, however, noted that -20 dB measured with both sources in the plane of maximum response seems to be the minimum practical signal-to-interference ratio for the parameters used in this study.

4.4 Effect of Clipping After Beamforming

The case of clipping after the beamforming process displays two phenomena. One concerns the interference signal when it is presented alone, the other concerns the combination of signal and interference. Each of these effects controls the shape of a different part of the

polar response of the array-spectrum analyzer combination. In order to facilitate comparison, the simulation clips after beamforming at the value input times the sum of the element weighting coefficients giving an effective clipping level equivalent to that used in the other cases.

Consider the action of the receiver with clipping after beamforming on the interference signal alone. The beamformer rejects this signal as it moves out of the beampattern in a normal manner. When the beamformer output level is beneath the clipping level, the system output is as it would be if no clipping were present. When the beamformer output level exceeds the clipping level, the spectrum level at the interference frequency is the clipping level. The skirts of this peak, as well as the maximum value, remain at a constant level as the strength of the interference increases with decreasing angle. This is important since it is the value of the skirt of the interference peak at the signal frequency that contributes to the signal peak height in the ratio spectrum. It is an extremely important property of a limiter for this discussion that, while limiting is taking place, the output power of the device approaches a constant (and is constant for hard limiting). Hence, when the interference amplitude exceeds the limiting amplitude, the excess energy which is clipped from the interference frequency goes into harmonics which are removed by the filter. The result is that the directivity of the line array-beamformer combination with respect to the interference signal alone consists of two distinct kinds of region. At those angles for which the beamformer output is below the clipping level, the response is identical to that for a system

in which no clipping is present. At angles for which the beamformer output is above the clipping level, the response is constant at the clipping level. If plotted, such a curve of interference rejection looks like a directivity plot for an unclipped system with its top cut off at the clipping level (e.g., Figure 4.7).

The action of the clipped-after beamforming array-spectrum analyzer combination on the signal plus interference depends upon the signal-to-interference ratio. If the signal is much larger than the interference, the signal dominates the clipper output. This is to say that the clipper output level at the signal frequency remains relatively constant as the interference level varies. Hence, if the output of the beamformer contains a signal component much larger than the interference, the variation in the signal level in the ratio spectrum will be due almost entirely to the variation in background level rather than to variation in the signal peak height in the signal-plus-interference spectrum.

If, however, the interference level is greater than the signal level so that the interference dominates the clipper maximum response, the reverse effect occurs as the interference moves out of the beampattern. As it moves, the interference is attenuated by the beamformer so that the signal becomes larger relative to the interference. The total output power of the clipper remains fairly constant (depending on the degree of clipping), but a larger percentage of the power is at the signal frequency. If the background spectrum is held constant, the signal level in the ratio spectrum falls off with increasing angle approximately as the main lobe of an unclipped directivity pattern until the interference becomes sufficiently small

that the signal dominates the clipper output and gives a constant output level at the signal frequency. It appears from simulation data that the constant signal spectral level is reached when the interference is approximately 5 dB below the signal level at the output of the beamformer.

The net result of these phenomena is that the directional response of the array-spectrum analyzer combination depends upon both the clipping level and the input signal-to-interference level. The existence and size of the main lobe depends upon the input signal-to-interference ratio (in dB) being negative. The side lobes will be flat unless the maximum rejection of the line is greater than the interference level minus the clipping level (both in dB). Hence, if the signal-to-interference ratio is positive and the clipping is quite hard, the directional response will be constant, i.e., there will be no directionality.

Two examples of the effects of clipping after beamforming are shown in Figures 4.6 through 4.9. Figures 4.6 and 4.7 are somewhat different from the other examples in this discussion in that the individual elements of the line were assumed to have a directional response given by:

$$f(\theta) = \frac{1.1 + \cos 2\theta}{2.1} \qquad (4.1)$$

which is a figure-eight pattern with approximately 26 dB attenuation at 90°. This extra attenuation helps to demonstrate both effects discussed above. The signal in this case is 20 dB below the interference, and the clipping level is 20 dB lower still. In Figure 4.8, the normalized response of the system to the interference alone

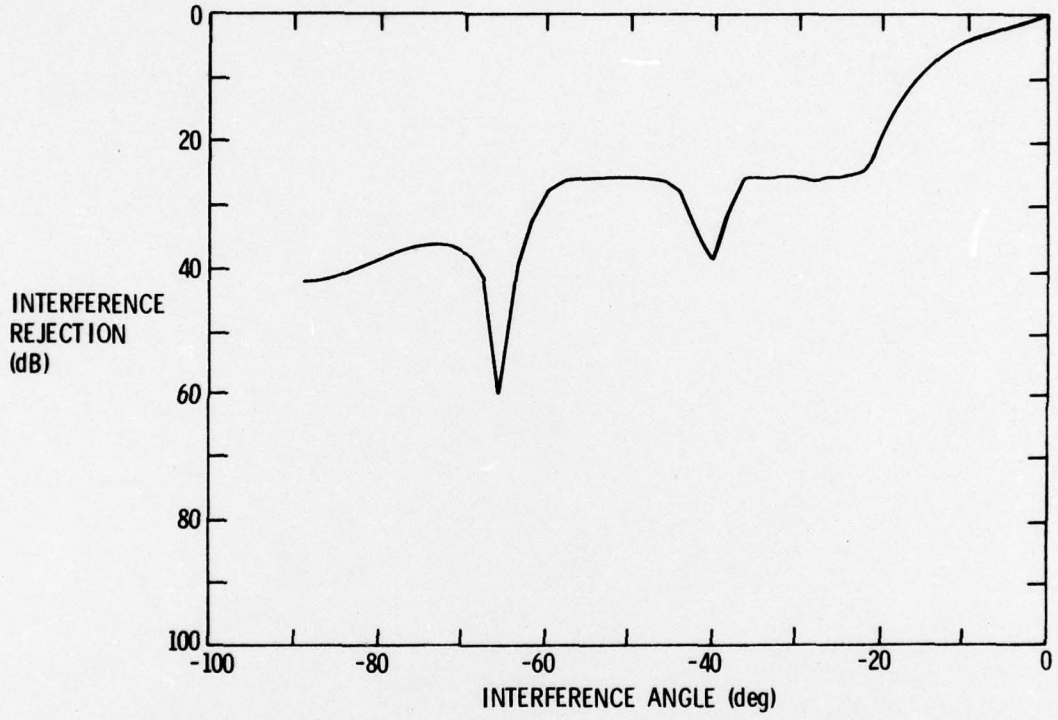

Figure 4.6 Directivity of the array with clipping after beamforming, Case I, signal 20 dB below interference and clipping 60 dB below interference.

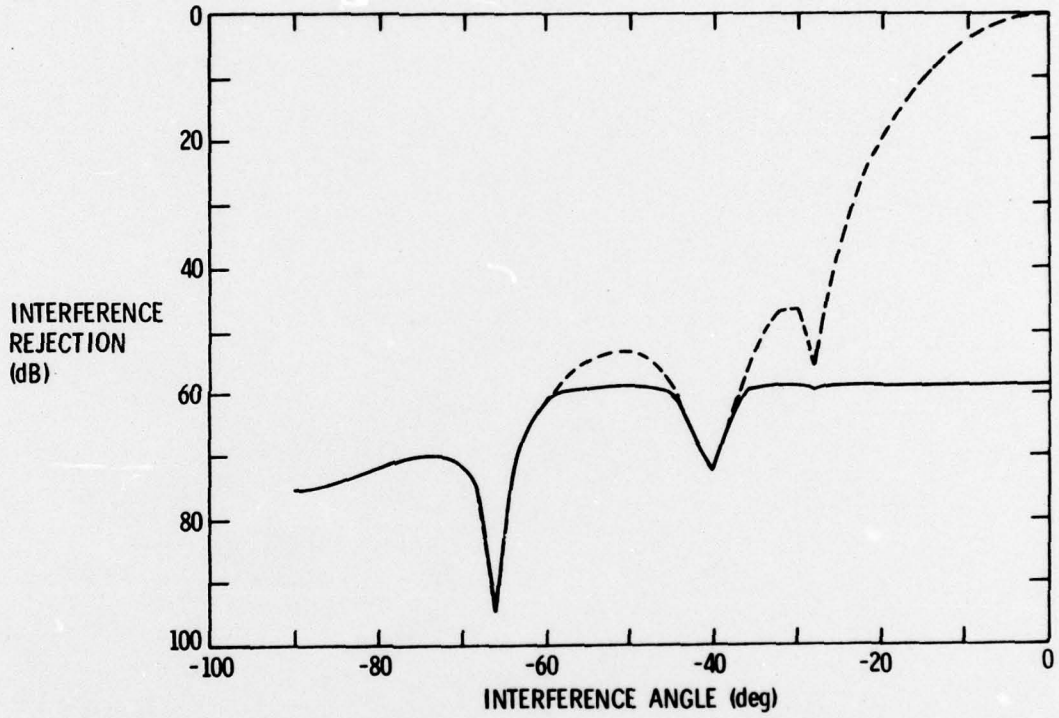

Figure 4.7 Rejection of the interference with clipping after beamforming, Case I. Solid: clipped 60 dB below interference level. Dotted: unclipped. Aligned to show similarity in shape.

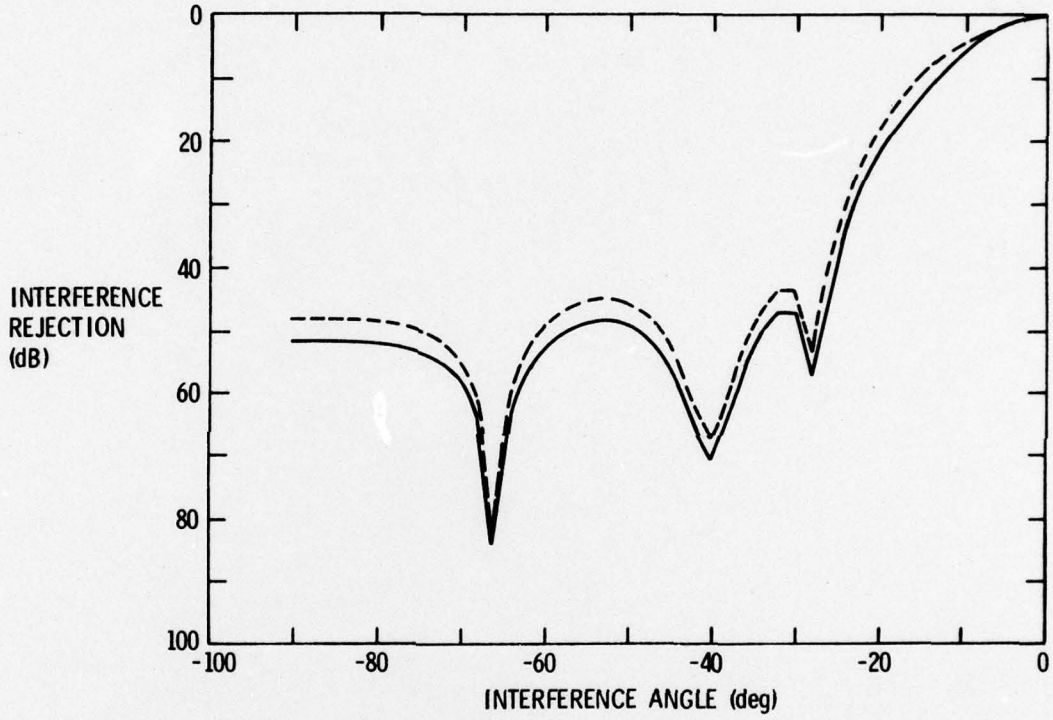

Figure 4.8 Directivity of the array with clipping after beamforming, Case II, signal 6 dB below interference and clipping 3 dB below interference (solid line). The dotted line is an unclipped case. This is an anomalous case in which clipping after beamforming yields slightly better rejection than no clipping at all.

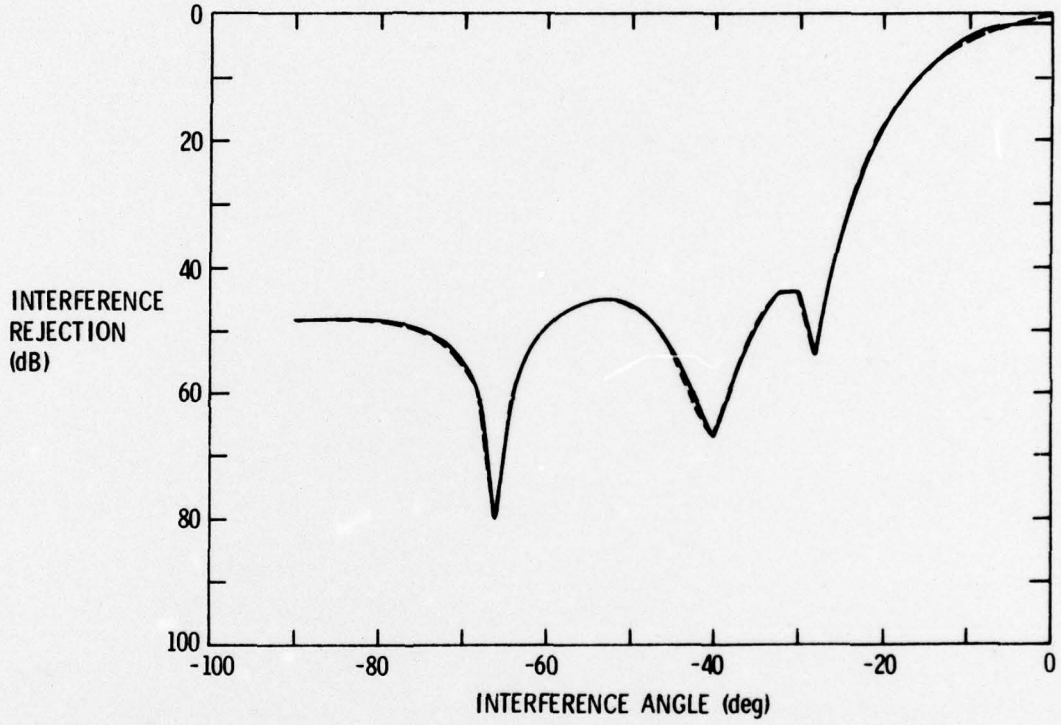

Figure 4.9 Rejection of the interference with clipping after beamforming, Case II. Solid: clipped 3 db below interference level. Dotted: unclipped.

as a function of angle is shown plotted with a similar plot for an unclipped case for signals below the clipping level (60 dB down). Except for a small transition region, the output level at all angles for which the input to the clipper is above the clipping level is held at the clipping level.

In its side-lobe region, Figure 4.6, the overall response, is shaped identically to Figure 4.8. This is because the signal is dominant when the interference is out of the plane of maximum response. The apparent main lobe in Figure 4.6 arises from the gradual shift in power at the clipper output from the interference frequency to the signal frequency as the interference moves. The height of this main lobe is equal to the interference-to-signal ratio plus about 5 dB.

Figure 4.8 shows a case in which clipping after beamforming actually improves the directionality of the line slightly. In this case, the signal amplitude is one-half of the interference amplitude, and the clipping amplitude is 70.7 percent of the interference amplitude. The individual transducers are again omnidirectional as they are in all other cases but the preceding one. Figure 4.9 is comparable to Figure 4.7. It shows that clipping distorts the response to interference alone only within a few degrees of the plane of maximum response. This slight flattening is more than offset by the increase in level of the signal at the output of the clipper as the interference moves off axis (the second effect discussed above). Consequently, the net effect of clipping is a slight increase in the main lobe height. Unfortunately, it is not usually feasible to control both the signal and the interference levels, so deterioration

of the directivity pattern is more likely than of enhancement if clipping is allowed to occur after beamforming.

CHAPTER V

CONCLUSIONS

The results of this study reduce to three primary conclusions:

1. Clipping of any degree occurring prior to beamforming does not cause consequential deterioration of the directivity of a line array with linear beamformer if the correct signal detection criterion is used.
2. Variations of signal-to-interference ratio have little effect on the directivity of the system studied provided that the signal remains detectable.
3. Clipping after the beamformer gives rise to gross changes in the directivity of the system which are highly dependent upon the amplitudes of both the signal and the interference and upon the clipping level. In any practical situation, the possible variation in directionality is so great as to render the system worthless.

It is certain from the results of this study that if clipping must occur in a system such as the one studied with a line array, it should be made to occur at the transducer elements and not after the beamformer.

An important extension of the research presented here is the replacement of the sinusoidal interference source by a source of broadband noise. The author has completed preliminary work on this problem including the development of a scheme for simulating beamforming with bandlimited noise samples.

Two other studies of interest are the development of a detection algorithm suitable for detecting a signal in the presence of a cross-product which appears larger than the signal in the present spectrum analyzer output (as described in Section 3.1) and the analysis of the sensitivity of the simulation to variations in element spacing and element-to-element variations in clipping level.

BIBLIOGRAPHY

1. Blachman, N. M. "Effect of a Limiter Upon Signals in the Presence of Noise." IRE Transactions on Information Theory, IT-6 (March, 1960), 52.

2. Kuznetsov, P. I., Strantonovich, R. L., and Tikhonov, V. I. Nonlinear Transformations of Stochastic Processes. Translated by J. Wise and D. C. Cooper. Oxford:Pergamon Press, 1965.

3. Middleton, D. "Some General Results in the Theory of Noise Through Nonlinear Devices." Quarterly of Applied Mathematics, V (1948), 445-498.

4. Shutterly, H. B. "General Results in the Mathematical Theory of Random Signals and Noise in Nonlinear Devices." IEEE Transactions on Information Theory, IT-9 (April, 1963), 74-84.

5. Thomas, John B. An Introduction to Statistical Communication Theory. New York:John Wiley and Sons, 1969.

6. Tucker, G. D. "Linear Rectifiers and Limiters." Wireless Engineer, 29 (May, 1952), 128-137.

7. Van Vleck, J. H. and Middleton, D. "The Spectrum of Clipped Noise." Proceedings of the IEEE, 54 (January, 1966), 2-19.

8. Wainstein, L. A. and Zubakov, V. D. Extraction of Signals from Noise. Translated from Russian by Richard A. Silverman. Englewood Cliffs, N.J.:Prentice-Hall, Inc., 1962.

DISTRIBUTION

Commander (NSEA 09G32)
Naval Sea Systems Command
Department of the Navy
Washington, D. C. 20362 — Copies 1 and 2

Commander (NSEA 0342)
Naval Sea Systems Command
Department of the Navy
Washington, D. C. 20362 — Copies 3 and 4

Defense Documentation Center
5010 Duke Street
Cameron Station
Alexandria, VA 22314 — Copies 5 through 16